

Article

Effect of h-BN and Nano-SiO₂ Fillers on the High-Temperature Tribological Properties of PEEK/PI-Based Composites

Mengjiao Li ¹, Jingjing Yang ², Shengqi Ma ³, Gang Liu ¹, Hongru Yang ¹ and Jianan Yao ^{1,*}

¹ Shanghai High-Performance Fibers and Composites Center (Province-Ministry Joint), Center for Civil Aviation Composites, Donghua University, Shanghai 201620, China; 2210457@mail.dhu.edu.cn (M.L.); liugang@dhu.edu.cn (G.L.); 2200426@mail.dhu.edu.cn (H.Y.)

² Tianma Microelectronics Co., Ltd., Shanghai 200120, China; yjjs12345@163.com

³ Institute of Shandong Non-Metallic Materials, Jinan 250031, China; masq19@mails.jlu.edu.cn

* Correspondence: yjn@dhu.edu.cn

Abstract: PEEK is being used increasingly often in seals, bushings, bearings, and other moving parts due to its excellent mechanical and tribological properties. Herein, PEEK-based composites were prepared using PI as the organic filler and h-BN and nano-SiO₂ particles as the inorganic fillers. There was significant improvement in the tribological properties of PEEK at conditions above the glass transition temperature; the coefficient of friction of +20P/4B/4Si was stabilized at 0.06 at 200 °C and the wear rate was reduced by 60% compared to PEEK. The role played by the thermal conductivity of h-BN and the promotion of friction transfer film by nano-SiO₂ in improving the tribological properties of PEEK is illustrated. The modified composites exhibited stable mechanical and tribological properties over a wide temperature range, which is instructive for instrumentation and testing applications in harsh environments.

Keywords: PEEK; PI; h-BN; SiO₂; friction coefficient; wear



Citation: Li, M.; Yang, J.; Ma, S.; Liu, G.; Yang, H.; Yao, J. Effect of h-BN and Nano-SiO₂ Fillers on the High-Temperature Tribological Properties of PEEK/PI-Based Composites. *Lubricants* **2023**, *11*, 416. <https://doi.org/10.3390/lubricants11100416>

Received: 29 August 2023

Revised: 12 September 2023

Accepted: 18 September 2023

Published: 22 September 2023



Copyright: © 2023 by the authors. Licensee MDPI, Basel, Switzerland. This article is an open access article distributed under the terms and conditions of the Creative Commons Attribution (CC BY) license (<https://creativecommons.org/licenses/by/4.0/>).

1. Introduction

Polymer composites are being used increasingly often to make moving parts such as bushings, thrust bearings, gaskets, and dynamic seals that are lighter, quieter, and more self-lubricating than traditional metal materials [1]. The rapid development of equipment and technology poses severe challenges to the frictional wear performance of these moving parts, especially under extreme conditions [2,3]. Therefore, the development of wear-resistant polymer composites with low friction coefficients is essential to minimizing friction-induced heat and improving the reliability of moving parts [4]. Polyether ether ketone (PEEK) is one of the most commonly used polymers because of its outstanding chemical resistance, radiation resistance, mechanical properties, and tribological properties [5–7]. However, the application of pure PEEK is limited by the relatively large coefficient of friction and wear rate, especially at high temperatures, at which it is challenging to maintain stable tribological properties. For this reason, further improvement of the tribological properties of PEEK is imperative.

Numerous early studies have shown that modification of PEEK with SiO₂ [8], SiC [9], Si₃N₄ [10], and ZrO₂ [11] inorganic particles can significantly improve the hardness, dimensional stability, impact resistance, and wear resistance of PEEK. Nano-SiO₂ can overlap with the electron clouds of polymer compounds and form a spatial network structure, which improves the mechanical strength, wear resistance, and aging resistance of polymer materials. Zhang et al. [12] prepared PEEK-based composites with nano-SiO₂ particles using a ball milling technique. When nano-SiO₂ was added at 1 vol%, the friction coefficient was still high at 0.45, even though the wear rate decreased significantly. Molazemhosseini et al. [13] investigated the tribological properties of PEEK composites reinforced with short carbon fibers and surface-modified nano-SiO₂ particles. It was shown that the incorporation of

nano-SiO₂ protected the interface between the carbon fibers and the matrix and improved the wear resistance of the composites. Unlike one-dimensional silicon dioxide nanoparticles, hexagonal boron nitride (h-BN) has good thermal conductivity and specific lubricating properties [14]. Notably, the high thermal conductivity of h-BN can transfer the heat generated on the sliding surface, significantly reducing the specific wear rate of composites. Liu et al. [15] reported the positive effect of using h-BN nanometers on improving the frictional wear properties of PEEK. Tharajak et al. [16] sprayed mixed PEEK with h-BN powders using a thermal spray technique. They mentioned that under the appropriate content of h-BN, the wear rate was reduced at both room and high temperatures.

In addition to inorganic fillers, organic polymer fillers have also been considered for improving the wear resistance of PEEK. Polyimide (PI) is characterized by its particular imide ring structure, which gives it high thermal stability and good tribological properties. It has been widely used in aerospace [17], microelectronics [18], and in nano [19] and laser [20] applications, etc. Yan et al. [21] prepared a series of thermoplastic polyimide (TPI) PEEK-based blends using the hot press molding method. The addition of TPI increased the hardness and decreased the friction coefficient. They mentioned that the wear mechanism changes from abrasive to adhesive wear when the test temperature exceeds the glass transition temperature. The former study showed an excellent potential for organic polymers to work together with inorganic fillers to improve polymers' friction and wear properties. However, fewer studies have been conducted on the high wear resistance of PEEK/PI-based composites in high-temperature applications.

Based on the above facts, inorganic and organic fillers have positive effects on the improvement of tribological properties of PEEK. Therefore, this study prepared a series of composites using PI as inorganic filler and different ratios of h-BN and nano-silica as inorganic fillers. The thermal stability, mechanical properties, thermal conductivity, and tribological properties of the composites were evaluated. The tribological properties of the composites were investigated at room temperature and at 200 °C. The effects of inorganic and organic fillers on the tribological properties were investigated by examining the contact surfaces' temperature change, the friction surfaces' morphology, the elemental distribution, and the friction transfer film.

2. Materials and Experimental Procedure

2.1. Materials

PEEK, with a melt index of 40 g/10 min, a glass transition temperature of 143 °C, and a melting point of 343 °C, was obtained from Heilongjiang Hairuite Engineering Plastics Co., Ltd. (Jiamusi, China). Amber YS-13 PI, with a density of 1.40 and a glass transition temperature of 239 °C, was obtained from Shanghai Synthetic Resin Factory. h-BN, with a molecular weight of 24.84 g/mol, a density of about 2.29 g/cm³, and a particle size of 5–7 μm, was purchased from Tianyuan Chemical. Silicon dioxide nanoparticles (nano-SiO₂), with particle sizes of 50 nm, were obtained from Nanjing XFNANO Materials Tech Co., Ltd. (Nanjing, China).

2.2. Specimen Preparations

We used a METI-22/40 twin-screw extruder with a speed of 50 r/min, in which the temperature of each heating section was controlled between 360 °C and 390 °C, and granulation using a pelletizer took place.

All of the raw materials (PEEK, PI, h-BN, and nano-SiO₂) were dried in a vacuum-drying oven at 120 °C for 4 h. The dried natural materials were pre-mixed for 15 min each in a high-speed mixer according to the formula in Table 1 and then extruded using a METI-22/40 twin-screw extruder (Guangzhou Putong Experimental Analytical Instruments Co., Ltd., Guangzhou, China) with the heating section controlled at 350–380 °C and the speed set at 40 r/min. The pellets were processed using a TY-400 injection molding machine (Hangzhou Dayu Machinery Co., Ltd., Hangzhou, China) under 90–130 MPa injection pressure, 90% injection flow rate, 15 s injection time, and 60 s holding time.

Table 1. The feed ratio of PEEK-based composites.

Sample No.	PEEK (wt.%)	PI (wt.%)	h-BN (wt.%)	SiO ₂ (wt.%)
PEEK	100	-	-	-
+20P	80	20	-	-
+20P/2B/2Si	76	20	2	2
+20P/4B/2Si	74	20	4	2
+20P/4B/4Si	72	20	4	4

2.3. Measurements

Thermogravimetric analysis (TGA) was carried out via a Thermogravimetric Analyzer (TA Instruments, 550) under a nitrogen atmosphere from 100 to 800 °C at a heating rate of 10 °C/min, respectively. Thermal dynamic mechanical analysis (DMA) was performed using a solid analyzer (TA Instruments, Q800) from 50 to 400 °C at a scan rate of 5 °C/min, with an amplitude of 10 μm and a load frequency of 1 Hz. Differential scanning calorimetric (DSC) measurement was carried out in a Differential Scanning Calorimeter (TA instruments, 250) at a heating rate of 10 °C/min from 35 to 400 °C under an N₂ atmosphere. The TH 210 Shore hardness tester measured the hardness of composite materials. Each sample was measured three times to take the average value. Type 1A specimens were prepared according to GB/T 1040-2006, and the tensile properties of each specimen were tested at a rate of 10 mm/min using a model 5966 universal testing machine (INSTRON Instruments, USA) at room temperature and at 200 °C, respectively. The extensometer with an initial extension span of 50 mm was settled. All the data were obtained with an average value of five measurements. The thermal diffusion coefficient of each sample was measured according to the ASTM E1461 method using a laser thermal conductivity meter (LFA 467 Hyper Flash models). The size of the piece was φ10 mm × 1 mm, and the specimen was tested at 250 V with a pulse width of 600 μm at 25 °C, 50 °C, and 200 °C. At each temperature 3 flash points were taken.

The test conditions used in this paper refer to the working scenario of sliding bearings in construction machinery and the regulations of ASTM G 99-04. A multifunctional tribological wear tester (MT Tribo-Lab, Bruker, Germany) was used for tribological performance testing. The contact type of friction mating sub was a pin disk, for which the standard sample is a cylindrical pin body with a size of φ5.9 mm × 18.8 mm, and the metal friction sub-disk was 45# stainless steel with a size of φ50 mm × 10 mm. The initial surface roughness R_a of the steel disc was approximately 0.05–0.13 μm. Before the friction test, samples were pre-sanded using 500# and 1500# sandpaper and cleaned thoroughly with acetone. The test load was F_z = 18 N (0.5 MPa) and 36 N (1 MPa), with sample sliding on the disc at 200 r/min with a 20 mm rotational radii for 2 h. This was repeated three times to calculate the average friction coefficient and wear rate. All friction tests were conducted both at room temperature and under non-lubricated conditions at 200 °C. The formula [5] for the calculation is as follows:

$$Ws = \Delta M / (\rho \cdot F \cdot L) \quad (1)$$

where ΔM is the specimen's weight change (g) before and after the test, weighed using a balance (MS105DU Mettler-Toledo, Switzerland). ρ is the specimen's density (g/cm³) and was measured based on Archimedes' law. F is the load (N) applied on the polymeric pin. L is the total sliding distance (m). Each test was replicated thrice to calculate the average friction coefficient and wear rate. The contact surface of the composite material with the steel disc was probed using the FOTRIC Handheld 320+ series. The spray-gold-treated composites' microscopic morphology was observed using a field emission scanning electron microscope (Hitachi Regulus 8230), and the SEM-adopting voltage was set at 10 kV. The TFLs on the surface of the steel disc were observed at a magnification of 35 using a digital optical microscope (RH-2000 HIROX 3D super depth-of-field microscope, Japan).

3. Results

3.1. Thermal and Physical Properties of Composites

The comprehensive behavior of composites is shown in Figure 1. The decomposition temperature ($T_{d5\%}$) of the composite increased from 526 °C to 535 °C with the addition of PI, and it changed slightly after the introduction of filler, indicating that these composites possess excellent thermal stability (Figure 1a). The results of the thermomechanical properties tests showed an increase in the energy storage modulus at room temperature after the addition of PI to PEEK, and the modulus at room temperature continued to increase slightly after the addition of filler due to the rigid inorganic fillers (Figure 1b). Moreover, DSC obtained high glass transition temperatures (higher than 145 °C) for composites (Figure S1). Additionally, introducing PI increased the Shore hardness of PEEK composites to 80 D \pm 0.4 compared with the pure PEEK of 53 D \pm 1.0 (Figure 1c). PI has a rigid imine ring structure [22], so +20PI is harder than PEEK.

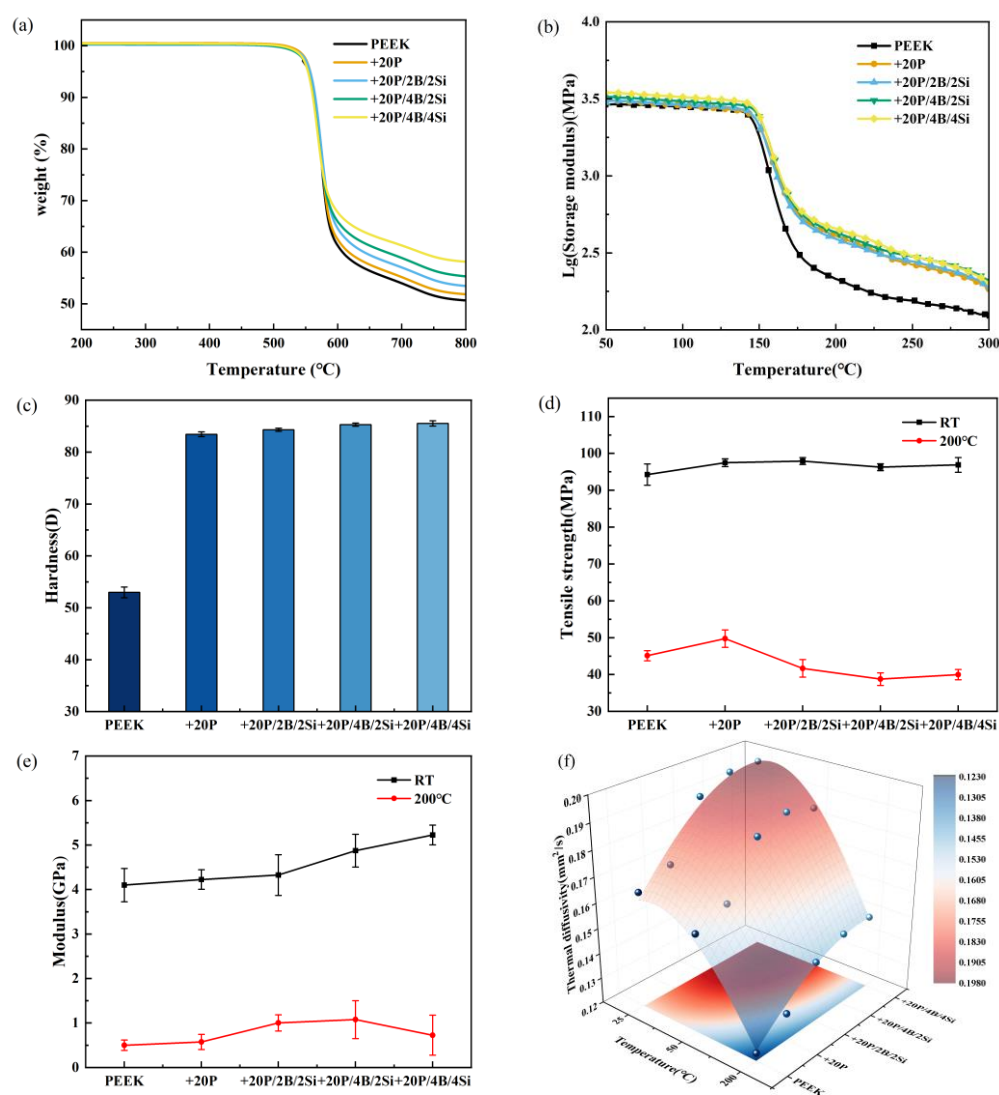


Figure 1. Comprehensive behavior of composites: (a) TGA, (b) DMA, (c) shore hardness, (d) tensile strength, (e) modulus, (f) conductivity of composites.

Further, the corresponding value of composites containing h-BN and nano-SiO₂ fluctuated from 83 D to 86 D. Inorganic particle-filled composites are subjected to greater external compressive loads, which favors wear resistance in friction. The relatively stable value showed the same trend as the former research [23,24]. The tensile strength and modulus of PEEK composites were higher above 90 MPa and 4 GPa under 25 °C (Figure 1d,e). The

fluctuation of mechanical properties in filler-contained composites was mainly attributed to the weak intermolecular force between the polymer matrix and fillers.

Moreover, these composites show excellent mechanical behavior under high-temperature conditions, in which +20P/2B/2Si possess the strength and modulus of 39 MPa and 1 GPa at 200 °C. In terms of the overall performance of the composites, the incorporation of PI and fillers maintains the thermal stability and hardness of the matrix at a high level. The strength of the composites did not fluctuate significantly due to the addition of the inorganic particles, and the increase in modulus meant that the material's resistance to deformation fracture was improved.

Figure 1f illustrates the thermal conductivity of PEEK and the composite from room temperature to 200 °C. Typically, the thermal diffusivity of the polymer is low. In this research, the thermal conductivity levels of PEEK and +20P were 0.16 mm²/s and 0.17 mm²/s at 25 °C. The introduction of h-BN resulted in a thermal diffusivity of more than 0.19 mm²/s for the complexes, indicating a significant role played by the graphene-like structure possessed by hexagonal boron nitride. Although the thermal diffusivity decreased with increasing temperature for all samples, the increasing trend in thermal conductivity brought by the fillers still had good retention. The thermal diffusivity levels of +20P/4B/2Si at 50 °C and 200 °C were 0.18 mm²/s and 0.15 mm²/s. The added PI further enhanced the heat transfer at the phase interface, as shown by the slight increase in thermal diffusivity. h-BN helped to conduct the heat generated on the surface in time during friction and avoided softening failure to a certain extent.

To further demonstrate the thermal conductivity played by h-BN, Figure 2 shows the friction surface's temperature change. The continuous heat generation and build-up of the material during the friction process can influence the morphology of the friction surface, which in turn affects its subsequent friction properties. The friction surface temperature increased as the test proceeded, with the PEEK showing temperatures of 39.1 °C and 52.8 °C before and after 80 min (Figure 2c,i). In addition, adding inorganic fillers reduced the temperature of the contact surface after friction (47.1 °C for +20P/4B/2Si). This phenomenon again proves that the introduction of h-BN diminishes the cumulative effect of heat during the friction process and thus improves the wear resistance of the composite.

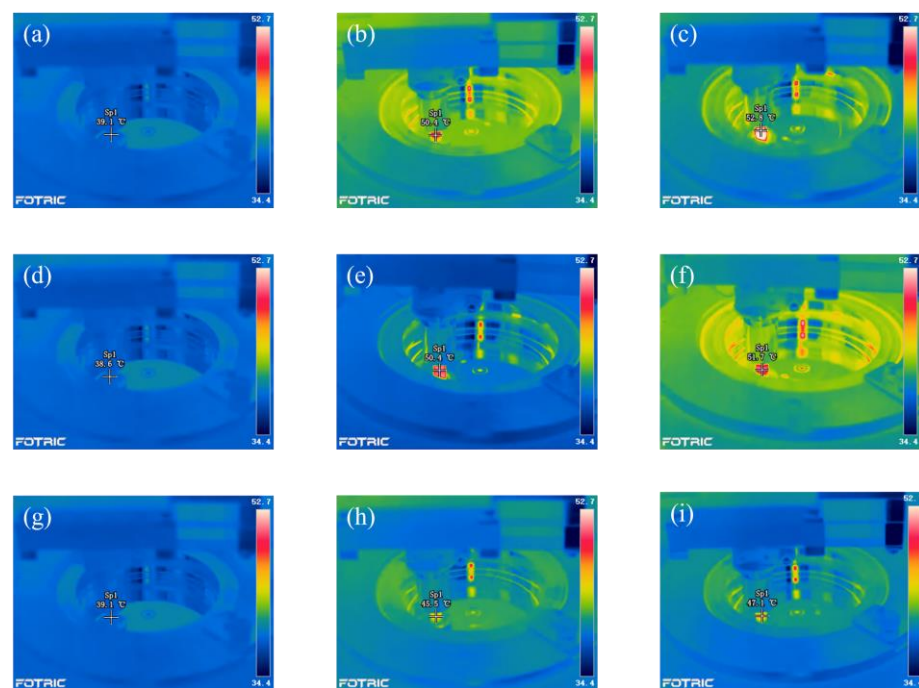


Figure 2. Infrared thermogram of friction surface at 0 min, 40 min, 80 min: (a–c) PEEK, (d–f) +20P, (g–i) +20P/4B/2Si.

3.2. Friction and Wear Properties of Composites

The friction coefficient and the wear rate of PEEK and composites at different loads varying with the test temperature are shown in Figure 3. The friction coefficient stabilizes with time for the dry friction of specimens against a metal ring at room temperature, as illustrated in Figure 3. Generally, the friction coefficient and the wear rate increase with increasing load. However, there is no significant difference in the coefficient of friction at a load of 0.5 MPa (Figure 3a,b). It is noticed that the friction coefficient for the PEEK composites sliding against the steel disks is reduced with an increase in temperature at 1 MPa. As seen from Figure 3c, the friction coefficient is relatively stable and remains constant at about 0.35 for the pure PEEK. PI does not substantially change the friction evolution tendency, whereas adding 20% PI increases the friction coefficient from 0.35 to about 0.52. As can be seen, incorporating 2% h-BN and 2% nano-SiO₂ could significantly reduce the friction coefficient of the +20PI. Adding h-BN and nano-SiO₂ into PEEK lowers the wear rate, gradually decreasing with enhancing h-BN from 2% to 4%. The wear rate of +20P/4B/2Si is reduced to 10×10^{-6} mm³/Nm. However, a further increment of the nano-SiO₂ content to 4% slightly increases the wear rate (Figure 3f).

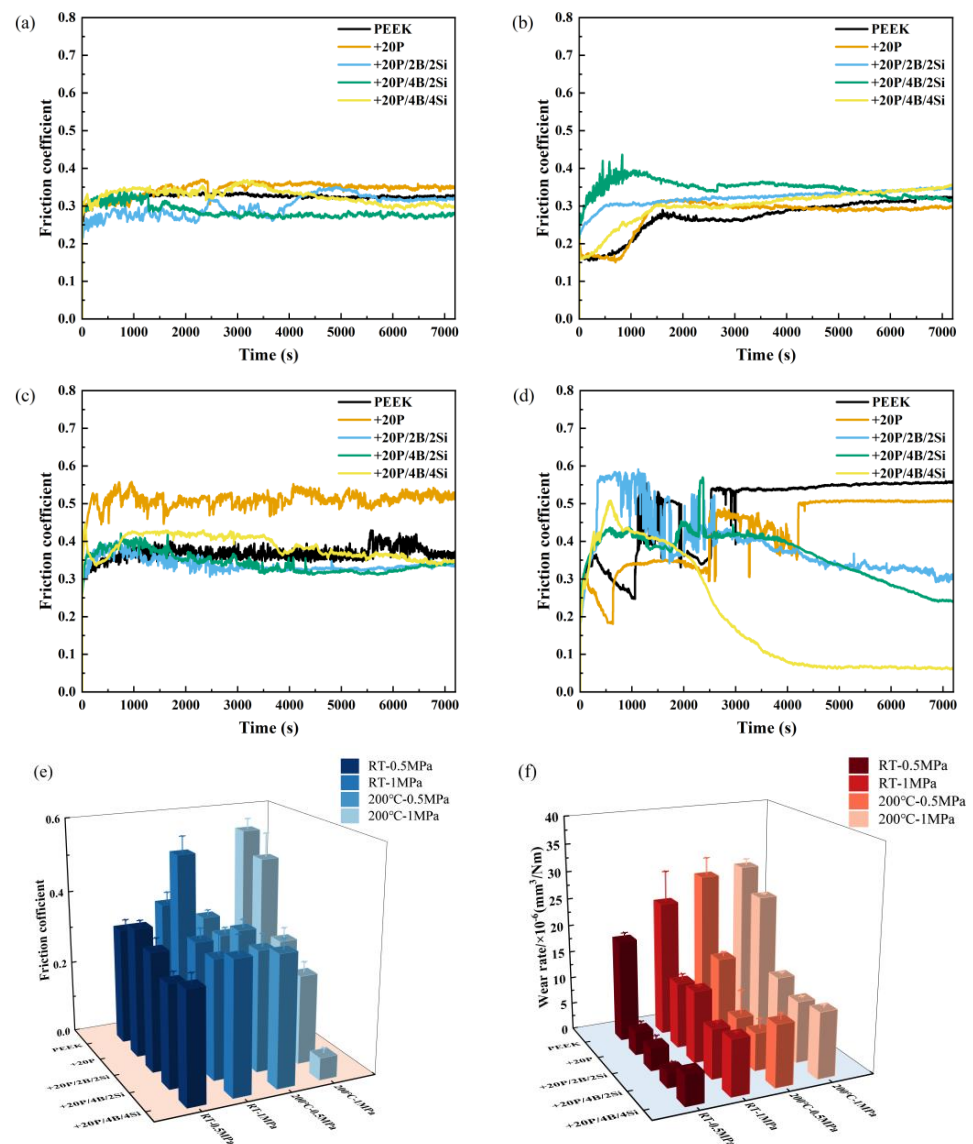


Figure 3. Friction and wear performance of composites: friction coefficient with the time at 0.5 MPa (a) room temperature and (b) 200 °C; 1 MPa at (c) room temperature and (d) 200 °C; (e) the friction coefficient and (f) wear rate of PEEK and composites.

As shown in Figure 3d, when the temperature increased to 200 °C, the friction coefficient of PEEK and +20P smoothed out after erratic fluctuations and remained high. However, the friction coefficient of composite materials gradually decreased after a period of unstable changes until it stabilized. With the addition of h-BN and nano-SiO₂, the friction coefficient of +20P/2B/2Si at 1 MPa decreased from 0.35 to 0.30. With the increasing content of h-BN and nano-SiO₂, the friction coefficient of +20P/2B/2Si and +20P/2B/2Si decreased from 0.32 and 0.34 to 0.21 and 0.08 (Figure 3e). Typically, the addition of complex fillers increased the wear rate of the composite at high temperatures. The wear rate did not increase significantly. Still, it fluctuated slightly between $10 \times 10^{-6} \text{ mm}^3/\text{Nm}$ and $12 \times 10^{-6} \text{ mm}^3/\text{Nm}$ (Figure 3f).

The hard inorganic particles plow against the softened substrate, and the wear fragments become finer under high temperatures, changing the wear mechanism from adhesive to abrasive wear. Moreover, the inorganic particles tend to be agglomerated with the chain movement of polymers. As the test proceeded, the size of the agglomerated particles increased and formed a friction transfer film with acceptable wear debris, thereby reducing the friction coefficient. The formation of the friction transfer film smoothed the friction surface and thus reduced the friction loss. This supposition will be verified further in detail via an investigation of the morphology of worn surfaces after wear tests with the help of an SEM and a digital optical microscope.

3.3. Microtopography and X-ray Photon Spectrum Analysis

As shown in Figures 4 and 5, the tested samples' surface morphology and elemental distribution were analyzed. Such flaking of PEEK chunks involved in friction indicates that adhesion is an important mechanism causing friction and wear (Figure 4a) [25]. The wear grooves on the +20PI surface were significantly reduced compared to pure PEEK (Figure 4b). In addition, no large pieces of peeling were observed from the wear marks of +20P/2B/2Si (Figure 4c). When the h-BN content was further increased from 2% to 4%, there was no significant increase in wear rate because the harder PI may have covered the h-BN to form protrusions to weaken the plowing effect (Figure 4c,d) [23]. In addition, the relatively homogeneous distribution of h-BN with thermal conductivity reduced the heat accumulation during the friction process, thus reducing the plowing phenomenon (Figure 4(e1)–(e3)).

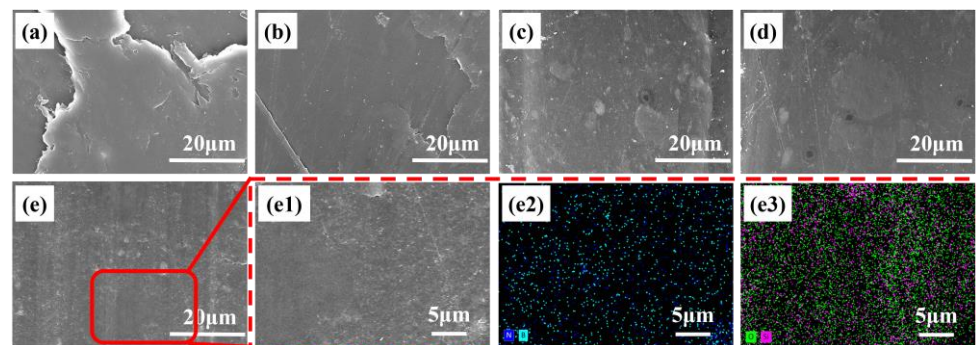


Figure 4. SEM: (a) PEEK, (b) +20P, (c) +20P/2B/2Si, (d) +20P/4B/2Si, (e) +20P/4B/4Si and EDS mapping images, (e1–e3) +20P/4B/4Si of worn composites surfaces at room temperature.

At 200 °C, the wear mechanism of PEEK (Figure 5a) and +20P (Figure 5b) was adhesive wear, and the friction surface remained extensively deboned. Adding inorganic particles made the wear surface significantly smoother (Figure 5c–e). In addition to the thermal conductivity of h-BN, agglomerations of nano-SiO₂ were observed on the friction surface (Figure 5(e3)), reducing the wear rate of composites significantly [26] and confirming the above analysis of the friction coefficients and the wear rates.

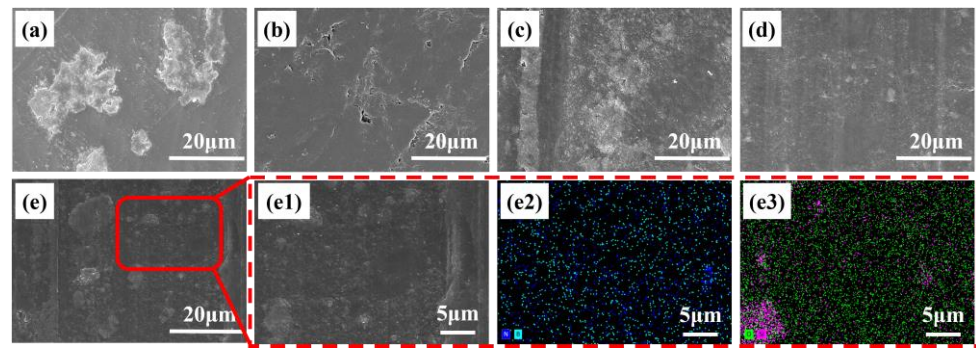


Figure 5. SEM: (a) PEEK, (b) +20P, (c) +20P/2B/2Si, (d) +20P/4B/2Si, (e) +20P/4B/4Si and EDS mapping images, (e1–e3) +20P/4B/4Si of worn composite surfaces at 200 °C.

Notably, the +20P/4B/4Si friction coefficient decreased substantially in the late friction period under 200 °C. Hence, it is necessary to investigate the chemical properties on the surface of the friction composite (Figure 6). For the O1s sub-peak, the firm signal peaks at 531.8 eV and 533.2 eV correspond to the chemical bond of C=O and C-O, respectively (Figure 6d). In addition, the elevation of Fe₂O₃ appears in the sub-peak of O1s, which indicates that the steel disk generates iron oxides during the friction and adheres to the surface of the composite. The oxide also plays a lubricating role in reducing the friction coefficient. After the friction test the relative content on the composite character of O1s increases, and that on C1s decreases. This phenomenon may be because the polymer molecules that break off at high temperatures chelate with their counterparts to form certain metal–organic compounds, which also become part of the friction-transfer film and reduce the coefficient of friction [27].

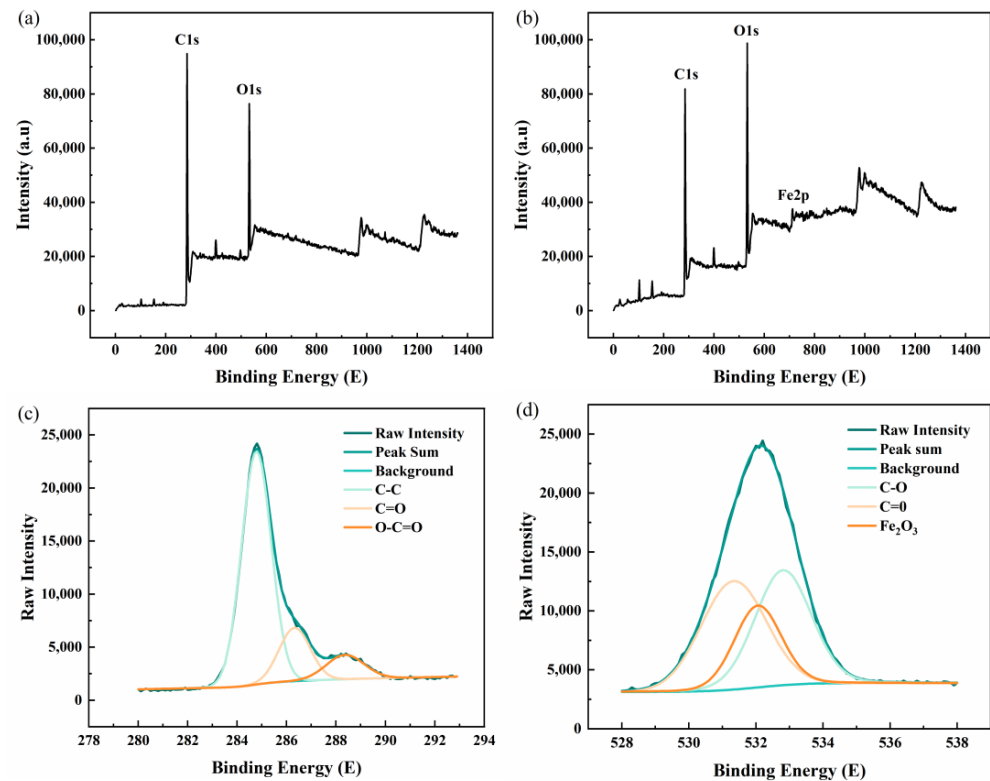


Figure 6. X-ray photon energy spectrum on the +20P/4B/4Si surface after wearing under 200 °C: (a) unworn, (b) after wear, and (c) C1s, (d) O1s.

3.4. Role of TFL Formation on Friction and Wear

The TFLs play an essential role in load transfer and can also improve material wear resistance in most tribological applications [28]. Figures 7, 8 and S2 systematically compared the TFLs on wear trajectories on steel discs. PEEK (Figures 7a and 8a) and +20P (Figures 7b and 8b) show the discontinuous TFLs on the steel disc surface at relative temperatures due to the heat accumulated during friction and the plasticization of the polymer surface [29,30]. In this case, the load-bearing capacity of the polymers decreased, leading to an easier dislodgement of polymer fragments and triggering severe wear [31]. Due to the positive effect of fillers on frictional transfer film formation, a relatively continuous transfer film was formed on the reverse side of +20P/4B/2Si (Figure 8c), which further proves the reduction in wear rate and friction coefficient [4,32]. Moreover, the TFLs showed darker under high temperatures than at room temperatures due to the stronger polymer chain movement. Remarkably, +20P/4B/4Si possesses a more uniform transfer film at 200 °C, indicating the positive effect of increasing nano-SiO₂ on improving wear resistance [24], echoing the agglomeration of nano-SiO₂ mentioned above (Figure 8d).

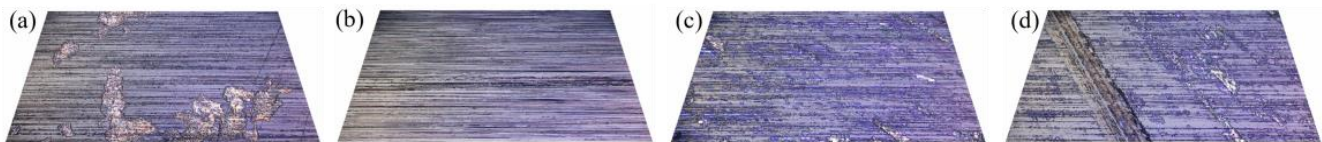


Figure 7. Three-dimensional microscope images of TFLs on steel disk after wear test at room temperature: (a) PEEK, (b) +20P, (c) +20P/4B/2Si, (d) +20P/4B/4Si.

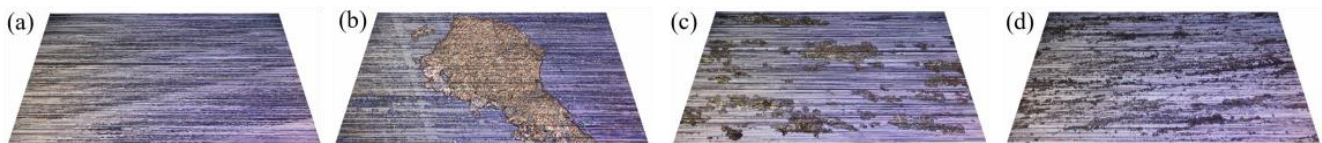


Figure 8. Three-dimensional microscope images of TFLs on steel disk after wear test at 200 °C: (a) PEEK, (b) +20P, (c) +20P/4B/2Si, (d) +20P/4B/4Si.

The evolution of the friction process of the composite on the steel disk at 200 °C is divided into three parts, as shown in Figure 9. The micro convexities on the metal surface come into contact with the micro convexities on the surface of the composite material, and the hard metal micro convexities deform and fracture the material, forming wear particles. This interaction will result in a slightly higher coefficient of friction, and as the friction process proceeds, debris doped with hexagonal boron nitride particles and silicon dioxide nanoparticles gradually builds up and sequentially transfers to the metal surface. Due to the nonpolar nature of the polymer, a uniform and thick TFL is formed under the combined effect of electrostatic attraction and mechanical stress. In adherence with this process, thermally conductive pathways were formed between the h-BN particles, attenuating the cumulative impact of friction-generated heat, as evidenced by a reduced wear rate [33]. In addition, hard nano-SiO₂ form because of the agglomeration effect so that the polymer molecules fracture and fall off, and chemical changes in the steel disk surface generate some metal–organic compounds. These substances are constantly sintered to form a friction transfer film, which reduces both the composite material and the friction vice of the actual contact area between the friction coefficient as friction is reduced [27].

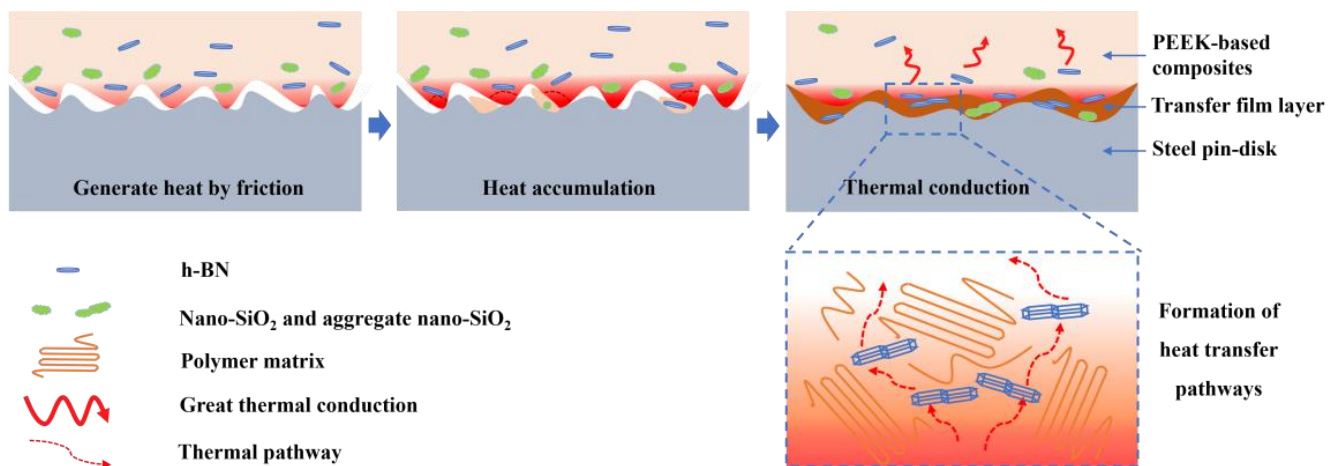


Figure 9. Schematic diagram of friction evolution stages of +20P/B/Si at 200 °C.

4. Conclusions

In summary, PEEK/PI-based composites with excellent wear resistance at elevated temperatures were obtained in this study. The composites possessed good thermal stability ($T_{d5\%}$ higher than 535 °C) and good mechanical behavior (tensile strength and modulus higher than 90 MPa and 4 GPa at room temperature). These composites exhibited a desirable friction coefficient (+20P/4B/4Si of 0.06) and wear rate at high temperatures. h-BN reduces the wear rate by reducing heat accumulation during friction due to its excellent thermal conductivity, suggesting that introducing high-thermal-conductivity fillers helps to improve the wear properties of the materials. In addition, the hard nano-SiO₂ reduces the contact area between the composite material and the friction partner due to its indirect promotional effect on the friction transfer film, which reduces the friction coefficient.

Furthermore, the morphology of the composite friction surface and the mechanisms of friction transfer film-generation were also demonstrated via a detailed analysis using SEM, EDS, XPS and digital optical microscopy. The results and comments provided in this study offer new insights into the design of high-performance, wear-resistant composites and new opportunities for their wide range of applications, such as in linings, gaskets, or in instruments for specific high-temperature testing environments.

Supplementary Materials: The following supporting information can be downloaded at: <https://www.mdpi.com/article/10.3390/lubricants11100416/s1>, Figure S1: Differential Scanning Calorimetry (DSC) scans of PEEK-based composites. Figure S2: 3D Microscope images of TFLs on steel disk after wear test of +20P/2B/2Si at (a) room temperature and (b) 200 °C.

Author Contributions: Data curation, M.L., J.Y. (Jingjing Yang) and H.Y.; Methodology, M.L., J.Y. (Jingjing Yang) and S.M.; Resources, G.L.; Supervision, G.L. and J.Y. (Jianan Yao); Writing—original draft, M.L.; Writing—review and editing, M.L., S.M. and J.Y. (Jianan Yao). All authors have read and agreed to the published version of the manuscript.

Funding: This research received no external funding.

Data Availability Statement: The data presented in this study are available on request from the corresponding author.

Acknowledgments: Thanks for the technical assistance from the Center for Civil Aviation Composites of Donghua University is greatly appreciated. This research received no funding.

Conflicts of Interest: The authors declare no conflict of interest.

References

1. Friedrich, K. Polymer composites for tribological applications. *Adv. Ind. Eng. Polym. Res.* **2018**, *1*, 3–39. [[CrossRef](#)]
2. Gackowski, B.M.; Phua, H.; Sharma, M.; Idapalapati, S. Hybrid additive manufacturing of polymer composites reinforced with buckypapers and short carbon fibres. *Compos. Part Appl. Sci. Manuf.* **2022**, *154*, 106794. [[CrossRef](#)]
3. Sajan, S.; Philip Selvaraj, D. A review on polymer matrix composite materials and their applications. *Mater. Today Proc.* **2021**, *47*, 5493–5498. [[CrossRef](#)]
4. Nunez, E.E.; Gheisari, R.; Polycarpou, A.A. Tribology review of blended bulk polymers and their coatings for high-load bearing applications. *Tribol. Int.* **2019**, *129*, 92–111. [[CrossRef](#)]
5. Song, J.; Liao, Z.; Shi, H.; Xiang, D.; Liu, Y.; Liu, W.; Peng, Z. Fretting Wear Study of PEEK-Based Composites for Bio-implant Application. *Tribol. Lett.* **2017**, *65*, 150. [[CrossRef](#)]
6. Wu, T.; Zhang, X.; Chen, K.; Chen, Q.; Yu, Z.; Feng, C.; Qi, J.; Zhang, D. The antibacterial and wear-resistant nano-ZnO/PEEK composites were constructed by a simple two-step method. *J. Mech. Behav. Biomed. Mater.* **2022**, *126*, 104986. [[CrossRef](#)]
7. Zhu, J.; Xie, F.; Dwyer-Joyce, R.S. PEEK Composites as Self-Lubricating Bush Materials for Articulating Revolute Pin Joints. *Polymers* **2020**, *12*, 665. [[CrossRef](#)]
8. Hou, X.; Hu, Y.; Hu, X.; Jiang, D. Poly (ether ether ketone) composites reinforced by graphene oxide and silicon dioxide nanoparticles. *High Perform. Polym.* **2017**, *30*, 406–417. [[CrossRef](#)]
9. Ghosh, S.; Dunnigan, R.; Gupta, S. Synthesis and tribological behavior of novel wear-resistant PEEK–Ti₃SiC₂ composites. *Proc. Inst. Mech. Eng. Part J J. Eng. Tribol.* **2016**, *231*, 422–428. [[CrossRef](#)]
10. Balaji, V.; Tiwari, A.N.; Goyal, R.K. Fabrication and properties of high performance PEEK/Si₃N₄ nanocomposites. *J. Appl. Polym. Sci.* **2011**, *119*, 311–318. [[CrossRef](#)]
11. Guo, L.; Qi, H.; Zhang, G.; Wang, T.; Wang, Q. Distinct tribological mechanisms of various oxide nanoparticles added in PEEK composite reinforced with carbon fibers. *Compos. Part A Appl. Sci. Manuf.* **2017**, *97*, 19–30. [[CrossRef](#)]
12. Zhang, G.; Schlarb, A.K.; Tria, S.; Elkedim, O. Tensile and tribological behaviors of PEEK/nano-SiO₂ composites compounded using a ball milling technique. *Compos. Sci. Technol.* **2008**, *68*, 3073–3080. [[CrossRef](#)]
13. Molazemhosseini, A.; Tourani, H.; Khavandi, A.; Eftekhari Yekta, B. Tribological performance of PEEK based hybrid composites reinforced with short carbon fibers and nano-silica. *Wear* **2013**, *303*, 397–404. [[CrossRef](#)]
14. Zeng, H.; Zhi, C.; Zhang, Z.; Wei, X.; Wang, X.; Guo, W.; Bando, Y.; Golberg, D. “White Graphenes”: Boron Nitride Nanoribbons via Boron Nitride Nanotube Unwrapping. *Nano Lett.* **2010**, *10*, 5049–5055. [[CrossRef](#)] [[PubMed](#)]
15. Liu, L.; Xiao, L.; Li, M.; Zhang, X.; Chang, Y.; Shang, L.; Ao, Y. Effect of hexagonal boron nitride on high-performance polyether ether ketone composites. *Colloid Polym. Sci.* **2015**, *294*, 127–133. [[CrossRef](#)]
16. Tharajak, J.; Palathai, T.; Sombatsompop, N. Recommendations for h-BN loading and service temperature to achieve low friction coefficient and wear rate for thermal-sprayed PEEK coatings. *Surf. Coat. Technol.* **2017**, *321*, 477–483. [[CrossRef](#)]
17. Samyn, P.; Schoukens, G.; De Baets, P. Micro- to nanoscale surface morphology and friction response of tribological polyimide surfaces. *Appl. Surf. Sci.* **2010**, *256*, 3394–3408. [[CrossRef](#)]
18. Xu, H.; Chen, W.; Wang, C.; Jia, T.; Wang, D.; Li, G.; Zhao, D.; Cui, B.; Fan, Z.; Fan, X.; et al. Ultralight and flexible silver nanoparticle-wrapped “scorpion pectine-like” polyimide hybrid aerogels as sensitive pressor sensors with wide temperature range and consistent conductivity response. *Chem. Eng. J.* **2023**, *453*, 139647. [[CrossRef](#)]
19. He, M.; Tang, J.; Wang, Y.; Li, R.; Huang, L.; Wang, X.; Yu, J. Preparation and properties of PANI/PI composite fabrics with conductive nanofiber network structure. *Polymer* **2022**, *240*, 124498. [[CrossRef](#)]
20. Lv, M.; Zheng, F.; Wang, Q.; Wang, T.; Liang, Y. Effect of proton irradiation on the friction and wear properties of polyimide. *Wear* **2014**, *316*, 30–36. [[CrossRef](#)]
21. Yan, Y.; Meng, Z.; Xin, X.; Liu, H.; Yan, F. Tribological Behavior and Thermal Stability of Thermoplastic Polyimide/Poly (Ether Ether Ketone) Blends at Elevated Temperature. *J. Macromol. Sci. Part B* **2020**, *60*, 175–189. [[CrossRef](#)]
22. Hu, C.; Qi, H.; Yu, J.; Zhang, G.; Zhang, Y.; He, H. Significant improvement on tribological performance of polyimide composites by tuning the tribofilm nanostructures. *J. Mater. Process. Technol.* **2020**, *281*, 116602. [[CrossRef](#)]
23. Xie, C.; Wang, K. Synergistic modification of the tribological properties of polytetrafluoroethylene with polyimide and boron nitride. *Friction* **2020**, *9*, 1474–1491. [[CrossRef](#)]
24. Wang, Q.; Xue, Q.; Shen, W. The friction and wear properties of nanometre SiO₂. *Tribol. Int.* **1997**, *30*, 193–197. [[CrossRef](#)]
25. Zhang, G.; Chang, L.; Schlarb, A.K. The roles of nano-SiO₂ particles on the tribological behavior of short carbon fiber reinforced PEEK. *Compos. Sci. Technol.* **2009**, *69*, 1029–1035. [[CrossRef](#)]
26. Bahadur, S.; Schwartz, C. The effect of nanoparticle fillers on transfer film formation and the tribological behavior of polymers. *Frict. Wear Bulk Mater. Coat.* **2013**, 23–48.
27. Guo, L.; Pei, X.; Zhao, F.; Zhang, L.; Li, G.; Zhang, G. Tribofilm growth at sliding interfaces of PEEK composites and steel at low velocities. *Tribol. Int.* **2020**, *151*, 106456. [[CrossRef](#)]
28. Tanaka, K. Transfer of semicrystalline polymers sliding against a smooth steel surface. *Wear* **1982**, *75*, 183–199. [[CrossRef](#)]
29. Yamamoto, Y.; Hashimoto, M. Friction and wear of water lubricated PEEK and PPS sliding contacts. *Wear* **2004**, *257*, 181–189. [[CrossRef](#)]
30. Zhang, G.; Zhang, C.; Nardin, P.; Li, W.Y.; Liao, H.; Coddet, C. Effects of sliding velocity and applied load on the tribological mechanism of amorphous poly-ether-ether-ketone (PEEK). *Tribol. Int.* **2008**, *41*, 79–86. [[CrossRef](#)]

31. Bahadur, S.; Gong, D. The role of copper compounds as fillers in the transfer and wear behavior of polyetheretherketone. *Wear* **1992**, *154*, 151–165. [[CrossRef](#)]
32. Kurdi, A.; Kan, W.H.; Chang, L. Tribological behaviour of high performance polymers and polymer composites at elevated temperature. *Tribol. Int.* **2019**, *130*, 94–105. [[CrossRef](#)]
33. Wang, T.; Wang, M.; Fu, L.; Duan, Z.; Chen, Y.; Hou, X.; Wu, Y.; Li, S.; Guo, L.; Kang, R.; et al. Enhanced Thermal Conductivity of Polyimide Composites with Boron Nitride Nanosheets. *Sci. Rep.* **2018**, *8*, 1557. [[CrossRef](#)] [[PubMed](#)]

Disclaimer/Publisher's Note: The statements, opinions and data contained in all publications are solely those of the individual author(s) and contributor(s) and not of MDPI and/or the editor(s). MDPI and/or the editor(s) disclaim responsibility for any injury to people or property resulting from any ideas, methods, instructions or products referred to in the content.